Dynamical model of a new type of self-balancing tractor-trailer-bicycle

Wei Zhuang[1], *Gaoming* Li[1], *Ruixin* Zhang[1], *Xiao* Su[1], and *Yonghua* Huang[1,*]

[1]School of Mechanical and Electrical Engineering, Guilin University of Electronic Technology, Guilin, China, 541004

Keywords: Self-balancing tractor-trailer-bicycle, Dynamical model, Chaplygin equation.

Abstract. In this paper, we focused on a Self-Balancing Tractor-Trailer-Bicycle(TTB) and developed an under-actuated dynamical model for the system. The bicycle is characterized with two parts, that is a tractor and a trailer, and considering the nonholonomic constrains from no-slipping contacts of its three wheels and the flat ground, we presented a dynamical model for the bicycle by using Chaplygin equation. The model suggest that the TTB should be an under-actuated system with three DOF (degree of freedom) and there are two driving-torque inputs. An inverse dynamics and a virtual prototype simulations are given to demonstrate the correctness of the proposed dynamical model.

1 Introduction

Self-balancing bicycle is the combination of bicycle mechanism and balance control technology. For this kind of two-wheeled mechanism, on the one hand, it can satisfy ones' needs of convenient travelling and labor-saving due to its lightweight and flexible body; on the other hand, the bicycle riders hope in some case that it can balance automatically, which can get rid of the dependence on ones' "driving". So far, the research on the self-balancing bicycle can be grouped into two types: "without mechanical regulator" and "with mechanical regulator".

Researchers who focus on self-balancing bicycle without mechanical regulators include Jones[1], Tanaka[2], Kooijman[3], Huang[4,5], and Li[6], etc. These researchers believed that the unmanned bicycle can achieve the dynamic balance of the body by governing the handlebar turning and the wheels running without adding additional mechanical regulators.

In the literatures [4-5], Huang introduced the principle of instantaneous rotation axis to analyze the constraints of bicycle robots, and used Lagrange method to establish its dynamic model. Huang also designed a motion controller based on partial feedback linearization method, and finally gave some physical prototype experiments, e.g., in situ, circular motion, linear balanced walking, etc.

Researchers who study self-balancing bicycles with mechanical regulators include Lee[7], Bui[8], Liu[9], Jin[10], Yin[11], Kim[12], etc. These researchers designed

[*] Corresponding author: huangyonghuaxj@sina.com

mechanical adjusting devices of moving or rotating for their bicycles. They stressed the dominant role of the mechanical adjusting devices in maintaining the balance of the body. The balance adjustment mechanism includes inertial flywheel (or rotating rod, or pendulum rod), translation mass block, mechanical gyro, etc.

At present, the research of self-balancing bicycle is mostly focused on the self-balancing of the body, and few of them can pay attention to the problem of the payload capacity of the system. Since the self-balancing bicycle without mechanical regulator has a simpler structure, fewer driving motors, lighter weight, and of more energy-saving. The existing self-balancing bicycles usually adopt the narrow structure of two wheels arranged back and forth, and the wheelbase between their two wheels has an important impact on their balance performance. If the wheelbase increased for improving the load-carrying capacity, it may cause many unexpected problems aroused from the frame deformation and flexibility reduction, and it is easy to lead the bicycle to lose balance.

How to improve the payload capacity without reducing the balance performance of the system? Inspired by the multi-section train, we proposed a new self-balancing bicycle mechanism composed of two-wheel tractor and single-wheel trailer. This kind of two-section bicycle retains the advantages of the traditional bicycle body in structure. If a breakthrough can be made in balance theory and experiment, this kind of mechanism should become a new type of convenient road traffic tool.

The structure of a new tractor-trailer-bicycle (TTB) are described in details in this article, and its dynamic model of the system was developed seriously by using Chaplygin equation.

2 Mechanical structure

The TTB consists of roughly two parts: a tractor and a trailer, which is shown in Fig. 1~Fig. 2.

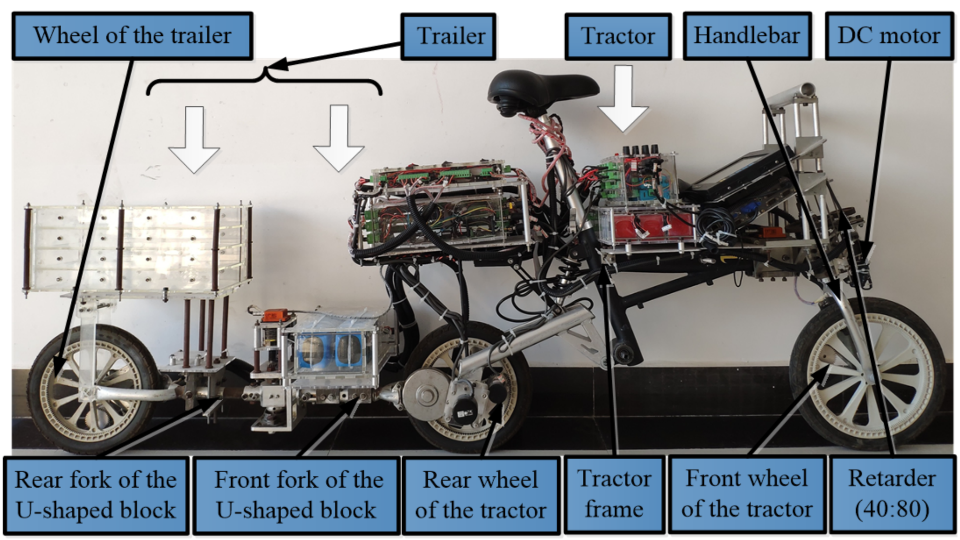

Fig. 1. Physical prototype of our TTB.

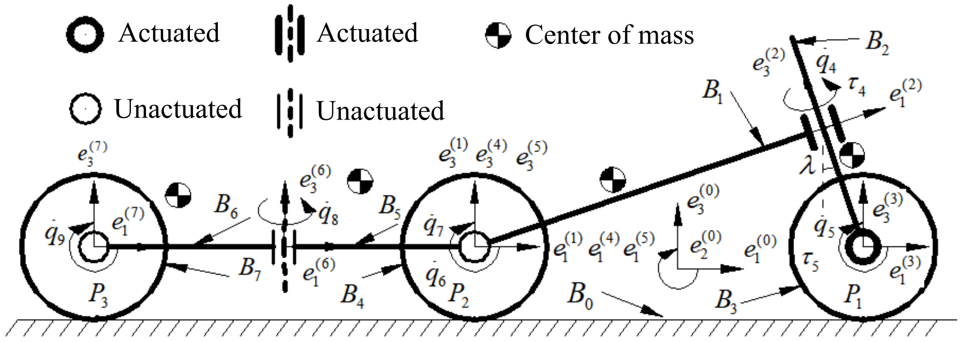

Fig. 2. Schematic diagram of our TTB.

As it is seen in Fig. 1~Fig. 2, the tractor includes a tractor frame, a handlebar, a front wheel of the tractor and a rear wheel. Both the handlebar and the rear wheel of the tractor are rotated around the frame, and the front wheel of the tractor rotates around the handlebar. The trailer comprises the front fork of the U-shaped block, the rear fork of the U-shaped block and the wheel. The front fork of the U-shaped block can be rotated up and down around the tractor frame, the rear fork of the U-shaped block can be rotated around the front fork of the U-shaped block, and the wheel of the trailer is rotated around the rear fork of the U-shaped block.

3 Dynamical model

3.1 Coordination settings

We denote the tractor frame by B_1, the handlebar by B_2, the front wheel of the tractor by B_3, the rear wheel of the tractor by B_4, the front fork of the U-block by B_5, the rear fork of the U-block by B_6, and the wheel of the trailer by B_7. The grounding point is denoted by P_1, P_2, and P_3. The coordinates of the Self-Balancing Tractor-Trailer-Bicycle are set to:

- $O-\boldsymbol{e}_1^{(0)}\boldsymbol{e}_2^{(0)}\boldsymbol{e}_3^{(0)}$ $\{0\}$ is the global coordinate system fixed on the ground;
- $O_1-\boldsymbol{e}_1^{(1)}\boldsymbol{e}_2^{(1)}\boldsymbol{e}_3^{(1)}$ $\{1\}$ is the coordinate system of the tractor frame B_1 and the origin of the coordinates is at the geometric center of the front wheel of the tractor B_3;
- $O_2-\boldsymbol{e}_1^{(2)}\boldsymbol{e}_2^{(2)}\boldsymbol{e}_3^{(2)}$ $\{2\}$ is the coordinate system of the handlebar B_2 and the origin of the coordinates is at the intersection of the frame of the tractor B_1 and the axis of the handlebar B_2;
- $O_3-\boldsymbol{e}_1^{(3)}\boldsymbol{e}_2^{(3)}\boldsymbol{e}_3^{(3)}$ $\{3\}$ is the coordinate system of the front wheel of the tractor B_3 and the origin of the coordinates is at the geometric center of the front wheel of the tractor B_3;
- $O_4-\boldsymbol{e}_1^{(4)}\boldsymbol{e}_2^{(4)}\boldsymbol{e}_3^{(4)}$ $\{4\}$ is the coordinate system of the rear wheel of the tractor B_4 and the origin of the coordinates is at the geometric center of the rear wheel of the tractor B_4;
- $O_5-\boldsymbol{e}_1^{(5)}\boldsymbol{e}_2^{(5)}\boldsymbol{e}_3^{(5)}$ $\{5\}$ is the coordinate system of the front fork of the U-shaped

block B_5 and the origin of the coordinates is at the geometric center of the rear wheel of the tractor B_4;

- $O_6 - \boldsymbol{e}_1^{(6)}\boldsymbol{e}_2^{(6)}\boldsymbol{e}_3^{(6)}$ $\{6\}$ is the coordinate system of the rear fork of the U-shaped block B_6 and the coordinate origin is at the intersection of the rear fork of the U-shaped block B_6 axis and the rotating shaft of the rear fork of the U-shaped block B_6 around the front fork of the U-shaped block B_5;
- $O_7 - \boldsymbol{e}_1^{(7)}\boldsymbol{e}_2^{(7)}\boldsymbol{e}_3^{(7)}$ $\{7\}$ is the coordinate system of the wheel of the trailer B_7 and the origin of the coordinates is at the geometric center of the wheel of the trailer B_7.

3.2 Constraint analysis

We suppose the bicycle was running on a flat plane, then the angular velocity of B_1 can be given as:

$$\boldsymbol{\omega}_{B1}^{(1)} = (c_3\dot{q}_2 - c_2 s_3 \dot{q}_1)\boldsymbol{e}_1^{(1)} + (s_2\dot{q}_1 + \dot{q}_3)\boldsymbol{e}_2^{(1)} + (c_2 c_3 \dot{q}_1 + s_3\dot{q}_2)\boldsymbol{e}_3^{(1)} \tag{1}$$

where $\boldsymbol{e}_i^{(j)}$ ($i = 1,2,3$, $j = 1,2,\cdots$) is the ith base vector of coordinate $\{j\}$. $s_i = \sin(q_i)$, $c_i = \cos(q_i)$ ($i = 1,2,\cdots$); $\dot{q}_i$ ($i = 1,2,3$) is the ith Euler angular rate of B_1 .

Because B_i ($i = 2,4,5$) rotates about B_1 , their angular velocity should be calculated as:

$$\boldsymbol{\omega}_{B2}^{(2)} = {}^2\boldsymbol{R}_1 \bullet \boldsymbol{\omega}_{B1}^{(1)} + \dot{q}_4 e_3^{(2)}, \quad \boldsymbol{\omega}_{Bi}^{(1)} = \boldsymbol{\omega}_{B1}^{(1)} + \dot{q}_{(i+2)} e_2^{(1)} (i = 4,5) \tag{2}\sim(4)$$

where ${}^j\boldsymbol{R}_i$ ($i, j = 1,2,\cdots$)denotes the rotation transform matric from the coordinate $\{j\}$ to $\{i\}$, and $\dot{q}_i$ ($i = 6,7$) denotes the angular rate of B_i ($i = 4,5$), respectively.

Because B_3 rotates around B_2 , B_6 rotates around B_5 , and B_7 rotates around B_6 , so the expressions of their angular velocity are as follows:

$$\boldsymbol{\omega}_{B3}^{(2)} = \boldsymbol{\omega}_{B2}^{(2)} + \dot{q}_5 e_2^{(2)}, \quad \boldsymbol{\omega}_{B6}^{(6)} = {}^6\boldsymbol{R}_1 \bullet \boldsymbol{\omega}_{B5}^{(1)} + \dot{q}_8 e_3^{(6)}, \quad \boldsymbol{\omega}_{B7}^{(6)} = \boldsymbol{\omega}_{B2}^{(2)} + \dot{q}_9 e_2^{(6)} \tag{5}\sim(7)$$

where $\dot{q}_i$ ($i = 4,5,8,9$) denotes the angular rate of B_i ($i = 2,3,6,7$), respectively.

Assume that the bicycle would not slide on the horizontal plane, so the speed of P_1 and P_2 is zero, then there we can get the following equation:

$$\boldsymbol{v}_{o3}^{(2)} + \boldsymbol{\omega}_{B3}^{(2)} \times ({}^2\boldsymbol{R}_3 \bullet r_1^{(3)}) = 0, \quad \boldsymbol{v}_{o4}^{(1)} + \boldsymbol{\omega}_{B4}^{(1)} \times ({}^1\boldsymbol{R}_4 \bullet r_2^{(4)}) = 0 \tag{8}\sim(9)$$

where $r_i^{(j)}$ ($i, j = 1,2,\cdots$) denotes the position vector of P_i in coordinate $\{j\}$.

In addition, there are the following equations:

$$\boldsymbol{v}_{o3}^{(2)} = {}^2\boldsymbol{R}_1 \bullet v_{o4}^{(1)} + \boldsymbol{\omega}_{B1}^{(1)} \times \boldsymbol{l}_{B3}^{(1)}, \quad \boldsymbol{v}_{o4}^{(4)} = \dot{x}\boldsymbol{e}_1^{(4)} + \dot{y}\boldsymbol{e}_2^{(4)} \tag{10}\sim(11)$$

where $l_{Bi}^{(j)}$ ($i = 1,2,\cdots,7; j = 1,5,6$)denotes the position vector in $\{j\}$ from the center of B_i to the origin of $\{j\}$, $v_{o4}^{(4)}$ is the linear velocity of the geometric center of the rear wheel of the tractor.

In (1)~(5) and (8)~(11), we can get the following four nonholonomic constraint equations:

$$\dot{q}_k = t_i\dot{q}_2 + t_{i+1}\dot{q}_4 + t_{i+2}\dot{q}_5 (k=1,6), \quad \dot{x} = f_1\dot{q}_2 + f_2\dot{q}_4 + f_3\dot{q}_5, \quad \dot{y} = f_4\dot{q}_2 \qquad (12)\sim(15)$$

Similarly, the speed of P_3 is zero, so we can get:

$$\dot{q}_k = v_i\dot{q}_2 + v_{i+1}\dot{q}_4 + v_{i+2}\dot{q}_5 (k=8,9) \qquad (16)\sim(17)$$

In (12)~(15), $\dot{x}$, $\dot{y}$ denote the longitudinal and the lateral velocity of the geometric center of B_4, respectively; and t_i, v_i, f_j ($i=1,4; j=1,2,3,4$)is the function of q_m ($m=2,3,4,7,8$).

In addition, considering the geometric constraints, we can get the following equations:

$$\begin{cases} ({}^0\boldsymbol{R}_1 \bullet {}^1\boldsymbol{R}_2 \bullet {}^2\boldsymbol{R}_3 \bullet (0,0,r_1))[3] = ((x_{C0}, y_{C0}, r_1c_2) + {}^0\boldsymbol{R}_1 \bullet \boldsymbol{l}_{B3}^{(1)})[3] \\ ({}^0\boldsymbol{R}_1 \bullet {}^1\boldsymbol{R}_5 \bullet {}^5\boldsymbol{R}_6 \bullet {}^6\boldsymbol{R}_7 \bullet (0,0,r_1))[3] = ((x_{C0}, y_{C0}, r_1c_2) + {}^0\boldsymbol{R}_1 \bullet {}^1\boldsymbol{R}_5 \bullet \boldsymbol{l}_{o6}^{(5)} + {}^0\boldsymbol{R}_1 \bullet {}^1\boldsymbol{R}_5 \bullet {}^5\boldsymbol{R}_6 \bullet \boldsymbol{l}_{B7}^{(6)})[3] \end{cases}$$

Eventually, we can derive the following two holonomic constraint equations:

$$\dot{q}_3 = w_1\dot{q}_2 + w_2\dot{q}_4, \quad \dot{q}_7 = ww_1\dot{q}_2 + ww_2\dot{q}_4 + ww_3\dot{q}_5 \qquad (18)\sim(19)$$

where r_1 denote the radius of three wheels, (x_{C0}, y_{C0}, r_1c_2) denote the position vector of the center of the rear wheel of the tractor in coordinate $\{0\}$, $(*)[3]$ is the 3rd item of the vector $*$, and w_i、ww_j ($i=1,2; j=1,2,3$) is the function of q_k ($k=2,3,4,7,8$).

We assume that the bicycle is running on a flat ground. The attitude matrix of the front fork of the U-shaped block is denoted by $\boldsymbol{R}_\alpha$, and the roll angle is denoted by α, and the attitude matrix of the rear fork of the U-shaped block is denoted by $\boldsymbol{R}_\beta$, and the roll angle is denoted by β. As a result, we would get two equations : $\boldsymbol{R}_a = {}^0\boldsymbol{R}_1 \bullet {}^1\boldsymbol{R}_5$, $\boldsymbol{R}_\beta = {}^0\boldsymbol{R}_1 \bullet {}^1\boldsymbol{R}_5 \bullet {}^5\boldsymbol{R}_6$. Therefore, we further have:

$$\alpha = q_2, \quad s_\beta = c_8s_2 + c_2s_8s_{3+7} \qquad (20)\sim(21)$$

From Eq. 16 and Eq. 18~Eq. 21, we can know α, β is the function of q_i ($i=2,4,5$).

3.3 Velocities of the COM

We set the velocity of the geometric center of B_4 as:

$$\boldsymbol{v}_{C4}^{(4)} = \dot{x}\boldsymbol{e}_1^{(4)} + \dot{y}\boldsymbol{e}_2^{(4)} \qquad (22)$$

Considering the principle of the relative motion, we can get the velocity of B_k ($k=1,2,3,5,6,7$), respectively, as follows:

$$\boldsymbol{v}_{Ci}^{(1)} = {}^{1}\boldsymbol{R}_{4} \bullet \boldsymbol{v}_{C4}^{(4)} + \boldsymbol{\omega}_{B1}^{(1)} \times \boldsymbol{l}_{Bi}^{(1)} \, (i=1,2,3), \quad \boldsymbol{v}_{C5}^{(1)} = {}^{1}\boldsymbol{R}_{4} \bullet \boldsymbol{v}_{C4}^{(4)} + \boldsymbol{\omega}_{B5}^{(1)} \times ({}^{1}\boldsymbol{R}_{5} \bullet \boldsymbol{l}_{B5}^{(5)}) \tag{23~26}$$

$$\boldsymbol{v}_{Cj}^{(1)} = {}^{1}\boldsymbol{R}_{4} \bullet \boldsymbol{v}_{C4}^{(4)} + \boldsymbol{\omega}_{B5}^{(1)} \times ({}^{1}\boldsymbol{R}_{5} \bullet \boldsymbol{l}_{o6}^{(5)}) + {}^{1}\boldsymbol{R}_{5} \bullet (\boldsymbol{\omega}_{B6}^{(6)} \times \boldsymbol{l}_{Bj}^{(6)}) \, (j=6,7) \tag{27~28}$$

where $\boldsymbol{v}_{Ci}^{(1)}$ is the velocity of B_i ($i=1,2,3,6,7$)in $\{1\}$, $\boldsymbol{l}_{o6}^{(5)}$ is the position vector in $\{5\}$ from the origin of $\{6\}$ to the origin of $\{5\}$.

3.4 Kinetic energy and potential energy

According to the derived $\boldsymbol{\omega}_{Bi}^{(j)}$ ($i,j=1,2,\cdots,5$) in Eq. 1~Eq. 7 and $\boldsymbol{v}_{Ci}^{(k)}$ ($i=1,2,\cdots,7; k=1,4$) in Eq. 22~Eq. 28, we can calculate the system's kinetic energy as:

$$T = \frac{1}{2}\sum_{i=1}^{5}((\boldsymbol{\omega}_{Bi}^{(j)})^T \boldsymbol{J}_{Bi} (\boldsymbol{\omega}_{Bi}^{(j)}) + (\boldsymbol{v}_{Ci}^{(k)})^T M_{Bi} (\boldsymbol{v}_{Ci}^{(k)})) \tag{29}$$

where $\boldsymbol{J}_{Bi}$ ($\boldsymbol{M}_{Bi}$)($i=1,2,\cdots,7$)represents the inertial matric(mass matrix)of B_i ($i=1,2,\cdots,7$), respectively.

By substituting the nonholonomic constrains Eq. 12~Eq. 17 into T , we will get another form of the kinetic energy $\tilde{T}$. Simultaneously, system gravity potential U can be given as:

$$U = \sum\nolimits_{i=1}^{7} m_i g h_i (i=1,2,\cdots,7) \tag{30}$$

where m_i and h_i are the mass and center height(the ground plane as the zero potential energy surface) of $B_i (i=1\sim 7)$, respectively. The formula of the height of each rigid body is as follows:

$$h_4 = r_1 c_2, \quad h_5 = h_4 + ({}^{0}R_1 \bullet {}^{1}R_5 \bullet l_{C_5}^{(5)})[3], \quad h_j = h_4 + ({}^{0}R_1 \bullet l_{C_j}^{(1)})[3] (j=1,2,3) \tag{31~35}$$

$$h_k = h_4 + ({}^{0}R_1 \bullet {}^{1}R_5 \bullet {}^{5}R_6 l_{C_6}^{(6)})[3] + ({}^{0}R_1 \bullet {}^{1}R_5 \bullet l_{o_k}^{(5)})[3] (k=6,7) \tag{36~37}$$

3.5 Dynamical model

Considering the following form of Chaplygin equation:

$$\frac{d}{dt}\frac{\partial \tilde{T}}{\partial \dot{q}_\sigma} - \frac{\partial \tilde{T}}{\partial q_\sigma} - \sum_{\beta=1}^{\gamma}\frac{\partial T}{\partial \dot{q}_{\varepsilon+\beta}}\sum_{\nu=1}^{\varepsilon}\left(\frac{\partial B_{\varepsilon+\beta,\sigma}}{\partial q_\nu} - \frac{\partial B_{\varepsilon+\beta,\nu}}{\partial q_\sigma}\right)\dot{q}_\nu = \tilde{Q}_\sigma \tag{38}$$

where T is the kinetic energy and $\tilde{T}$ is the kinetic energy by substituting nonholonomic constrains into T ; $B_{\varepsilon+\beta,\sigma}$ is the σth coefficient of the βth nonholonomic constrain; q_ν and q_σ are the generalized coordinates of the system; ε and γ are the numbers of the independent generalized coordinates and the nonholonomic constrains; $\tilde{Q}_\sigma$ is the σth generalized force of the system. The system's dynamics as:

$$\boldsymbol{D}(\boldsymbol{q})\ddot{\boldsymbol{q}}_\theta + \boldsymbol{C}(\boldsymbol{q},\dot{\boldsymbol{q}}_\theta)\dot{\boldsymbol{q}}_\theta + \boldsymbol{G}(\boldsymbol{q}) = \boldsymbol{\tau} \tag{39}$$

In (39), $\boldsymbol{C}(\boldsymbol{q},\dot{\boldsymbol{q}}_\theta)=\left(C_{ij}\right)_{3\times3}$, $\boldsymbol{G}(\boldsymbol{q})=\begin{pmatrix}G_1 & G_2 & 0\end{pmatrix}^T$, and $\boldsymbol{D}(\boldsymbol{q})=\left(D_{ij}\right)_{3\times3}$ denote centripetal-Coriolis, gravity terms and the inertia; $\boldsymbol{\tau} = (0,\tau_4,\tau_5)^T$ denote the driving torque vector; $\boldsymbol{q}_\theta$ and $\boldsymbol{q}$ are two kinds of generalized coordinates, which are defined as: $\boldsymbol{q}_\theta = \left(q_2,q_4,q_5\right)^T$, $\boldsymbol{q} = \left(q_1,q_3,q_7,q_8\right)^T$.

Eq. 39 indicates the TTB is an under-actuated system with three independent velocities, and for more detail: The roll angle (q_2、α、β) of B_1、B_5、B_6 are under-actuated,and α、β is the function of q_i ($i = 2,4,5$); There are totally two driving inputs in the two joints q_i ($i = 4,5$), so we could regulate control-force inputs τ_i ($i = 4,5$) of the two joints to control the roll angle (q_2、α、β) of the TTB.

4 Model verification

We will demonstrate the reliability of the model (see Eq. 39) by two different approaches. One is the use of an inverse dynamic simulation of Eq.39 under a given balanced trajectory in Matlab, from which we compare the energy increment with the input work of the dynamic bicycle. The other is the use of a virtual prototype simulation in ADAMS, by which we compare the driving torque of the handlebar in Adams with the model-calculated handlebar driving torque.

Table 1 shows the physical parameters which would be used in the numerical simulation. Note that we obtain the parameters from the measurement of a virtual TTB prototype in Solidworks.

Table 1. Physical parameters.

Symbol	Value	Unit	Symbol	Value	Unit	Symbol	Value	Unit
l_1	0.250	m	$l_{B7}^{(6)}$	$\begin{pmatrix}-0.347 & 0 & 0\end{pmatrix}$	m	m_1	25.038	kg
$l_{B1}^{(1)}$	$(0.275,0,0.145)$	m	J_{B1}	$\begin{pmatrix}3.106 & 0 & 0\\ 0 & 0.581 & 0\\ 0 & 0 & 2.629\end{pmatrix}$	kg·m2	m_2	2.946	kg
$l_{B2}^{(1)}$	$(0.070,0,0.166)$	m	J_{B2}	$\begin{pmatrix}0.070 & 0 & 0\\ 0 & 0.073 & 0\\ 0 & 0 & 0.008\end{pmatrix}$	kg·m2	m_w	1.616	kg
$l_{B3}^{(1)}$	$(0.893,0,0)$	m	J_{B3}	$\begin{pmatrix}1.000 & 0 & 0\\ 0 & 0.500 & 0\\ 0 & 0 & 1.000\end{pmatrix}$	kg·m2	m_5	2.294	kg
$l_{B5}^{(1)}$	$(-0.274,0,0.036)$	m	J_{B5}	$\begin{pmatrix}0.040 & 0 & 0\\ 0 & 0.070 & 0\\ 0 & 0 & 0.040\end{pmatrix}$	kg·m2	m_6	2.070	kg
$l_{B6}^{(6)}$	$(-0.204,0,0.102)$	m	J_{B6}	$\begin{pmatrix}0.033 & 0 & 0\\ 0 & 0.056 & 0\\ 0 & 0 & 0.060\end{pmatrix}$	kg·m2	r_1	0.200	m

4.1. Inverse dynamics simulations

The simulation is perform with two steps.

- **Step 1: trajectory planning**

We plan the motion trajectory of the roll angle of the tractor frame B_1 and the angular velocity of the front wheel of the tractor B_5:

$q_2 = A_1 e^{-\sigma t} \sin(\omega t + \varphi)$, $\dot{q}_5 = A_2$, $\ddot{q}_5 = 0$.

where $A_1 = \pi / 35$, $A_2 = 6\pi$, $\sigma =$ -1, $\omega = \pi$, $\varphi = \pi / 2$.

- **Step 2: : driving torque calculating**

By solving Eq. 39, we can calculate the driving torque τ_4 of the handlebar B_2 and the driving torque τ_5 of the front wheel of the tractor B_5, and then we will obtain:

$$\tau_4 = (D_{21} - \frac{D_{11}D_{22}}{D_{12}})\ddot{q}_2 - \frac{D_{11}F_1}{D_{12}} + F_2, \quad \tau_5 = (D_{31} - \frac{D_{11}D_{32}}{D_{12}})\ddot{q}_2 - \frac{D_{32}F_3}{D_{12}} + F_2 \tag{40}$$

Here, $F_1 = C_{11}\dot{q}_2 + C_{12}\dot{q}_4 + G_1$, $F_2 = C_{21}\dot{q}_2 + C_{22}\dot{q}_4 + G_2$, $F_3 = C_{31}\dot{q}_2 + C_{32}\dot{q}_4 + G_3$.

Fig. 3 examines two kinds of kinetic energy: T1 is get by the current velocity and T2 is get by the previous velocity and the elementary work.

Fig. 4 shows the difference between the mechanical energy and the work of the running bicycle.

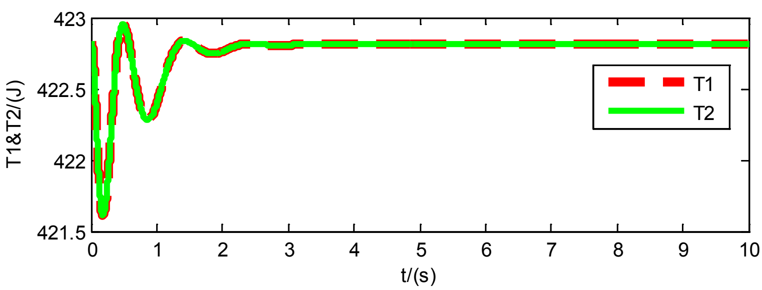

Fig. 3. Comparison of two kinds of kinetic energy.

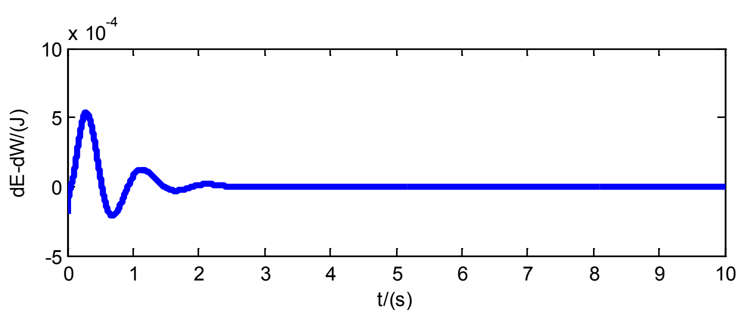

Fig. 4. Difference between energy and work.

As seen in Fig. 3~Fig. 4, while calculated by use of different variable, the two kinetic energy are coincident, and the difference between the increment of the mechanical energy and the elementary work is less than 10^{-3} (see Fig. 4). The results show that our dynamical model (Eq. 39) strictly obey the law of conservation of energy.

4.2. Virtual prototype simulation

The simulation is as follows:

- **Experiment description**

First, we build the virtual prototype in Adams platform, and add kinematic pairs and constraints to each rigid body part. Secondly, we define the type of contact between the wheels of the TTB and the ground, and add static friction and dynamic friction. The parameter settings such as system quality, moment of inertia, length and body structure length required for simulation are shown in Table 1.Finally, the angular velocity of the B_3 is set to 650r/min, then a simply PD controller is designed as:

$\tau_4 = k_{p1} q_2 + k_{d1} \dot{q}_2$, in which $k_{p1} = 15$, $k_{d1} = 5$.

The handlebar is governed by the controller to balance the TTB. The simulation continue with 20s due to the space limit. The relative data of the virtual prototype are exported for the post process after the complement of the simulation.

- **Experiments result and analysis**

We calculated the driving torque of the handlebar B_2 through the dynamical model in Eq. 39. Also, we got the measurement of this torque from ADAMS.

Fig. 5 show that TTB is running on a flat plane in the ADAMS simulation platform environment.

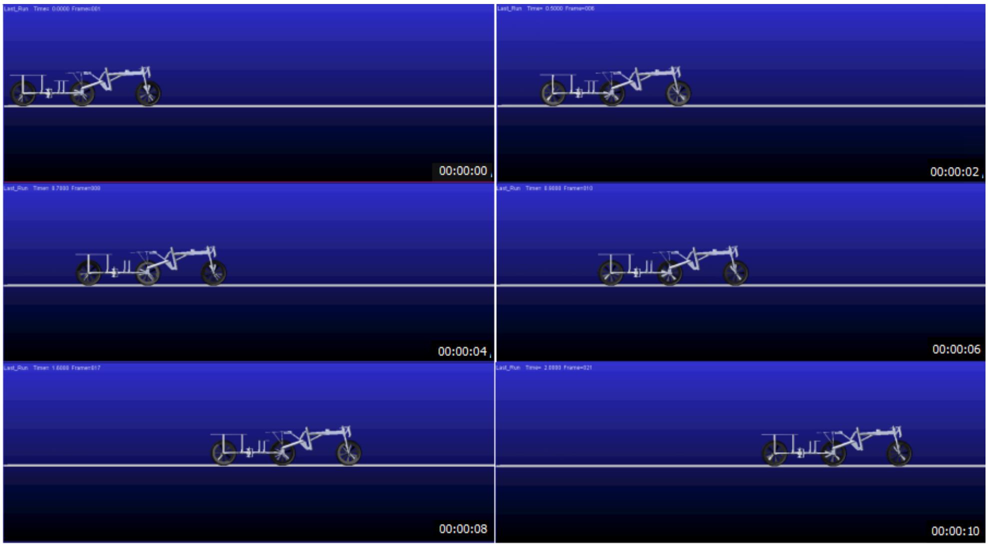

Fig. 5. Snapshot of the balanced running TTB in ADAMS.

Fig. 6 show the results of the analysis.

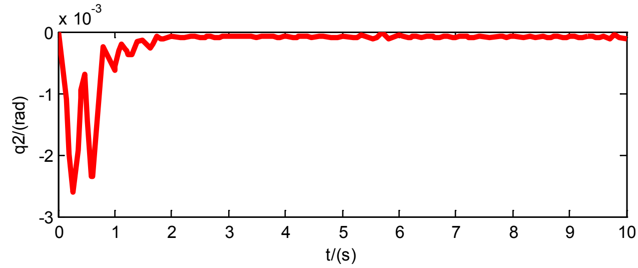

a) the roll angle of the tractor frame

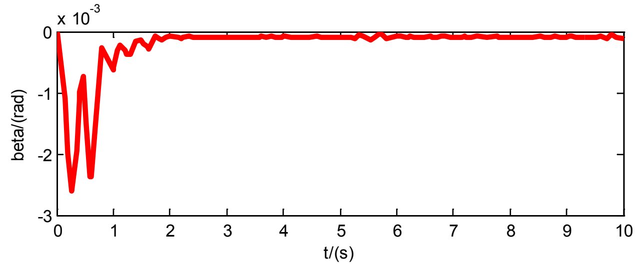

b) the roll angle of the rear fork of the U-block

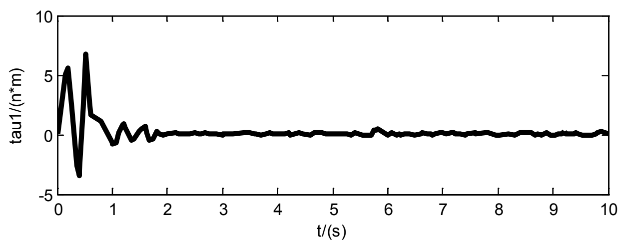

c) the angular acceleration of the front wheel of the tractor

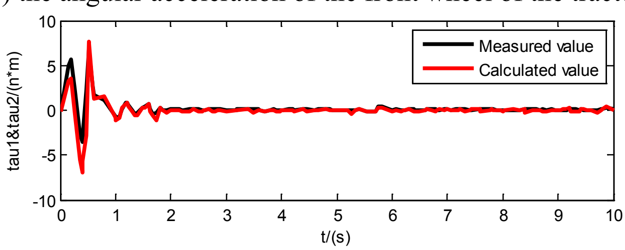

d) the driving torque of the handlebar

Fig. 6. The data to be exported in Adams.

It is illustrated that the two kinds of the driving torque of the handlebar B_2 exhibited the similar trend with a little difference in the amplitude. The reasons for the difference maybe as follows:

1) There definitely is wheel slippage because the angular acceleration of the front wheel of the tractor B_5 is relatively large form 0 to 0.5 second; 2) The measurement errors of virtual sensors; 3) The structural parameter measurement errors; 4) The proposed dynamical model is developed under ideal assumption without considering the friction between the wheels and the ground etc.

As a conclusion, the results of the two simulations seriously demonstrate the correctness and the reliability of the proposed dynamical model (Eq. 39).

5 Conclusions and future work

One of the contribution of this research is that we suggest that the TTB can be controlled balance by the handlebar. Another contribution of the research might be that we explored the dynamical model for the system. Our model illustrates that the TTB is explicitly a nonholonomic and under-actuated system, which consist of three independent velocities and two control-torque inputs. With the comparison between numerical and virtual prototype simulation, we validated that the reliability of our dynamical model. However, by so far, there is lack of realistic test to provide further support for our theoretical analysis; so, our next work should concentrate on the physical experiments.

Our work has received the financial support from National Natural Science Foundation of China (Grant No. 51765011 && No. 51865005) and Project of Guangxi Natural Science Foundation (Grant No. 2018JJA160115 && No. 2018JJA160116).

References

1. Jones D E H. The stability of the bicycle[J]. Physics Today, 1970, 23(4): 34-40.
2. Tanaka Y, Murakami T. Self sustaining bicycle robot with steering controller[C]// The 8th IEEE International Workshop on Advanced Motion Control, Kawasaki International Center, Kawasaki, Japan. Kawasaki: IEEE, 2004: 193-197.
3. Kooijman J D G, Meijaard J P, Papadopoulos J M. A bicycle can be self-stable without gyroscopic or caster effects [J]. Science Magazine, 2011, 332(6027): 339-342.
4. Huang Y H, Liao Q Z, Guo L, et al. Simple realization of balanced motions under different speeds for a mechanical regulator-free bicycle robot[J]. Robotica, 2014, 72(9): 1-15.
5. Huang Y H, Liao Q Z, Guo L, et al. Balanced motions realization for a mechanical regulators free and front-wheel drive bicycle robot under zero forward speed[J]. International Journal of Advanced Robotic Systems, 2013, 10(317):1-9.
6. Li J, Wei S M, Guo L, et al. Adaptive fuzzy control of a front-wheel drive bicycle robot[C]// 2016 4th International Conference on Cloud Computing and Intelligence Systems, IEEE, 2016: 113-116.
7. Lee S, Ham W. Self stabilizing strategy in tracking control of unmanned electric bicycle with mass balance[C]// Proceedings of the 2002 IEEE/RSJ International Conference on Intelligent Robots and Systems, Lausanne, Switzerland. Lausanne: IEEE, 2002: 2200-2205.
8. Bui T T, Parnichkun M, Le C H. Structure-specified H∞ loop shaping control for balancing of bicycle robots: A particle swarm optimization approach[J]. Proceedings of the Institution of Mechanical Engineers. Part I: Journal of Systems and Control Engineering, 2010, 224(7): 857-867.
9. Liu Y B, Jia C H, Han J H. Dynamics modeling of an unmanned bicycle with parallel mechanism adjusting stability[C]// Proceedings of the 2009 IEEE International Conference on Mechatronics and Automation, Changchun, China. Changchun: IEEE, 2009: 1601-1605.
10. Jin H Z, Yang D C, Liu Z X, et al. A gyroscope-based inverted pendulum with application to posture stabilization of bicycle vehicle[C]// Proceedings of the 2015 IEEE Conference on Robotics and Biomimetics, Zhuhai, China. Zhuhai: IEEE, 2015:2103-2108.

11. Yin S, Yamakita M. Passive velocity field control approach to bicycle robot path following [C]// Proceedings of the SICE Annual Conference, Tsukuba, Japan. Tsukuba : IEEE, 2016: 1654-1659.
12. Kim Y, Kim H, Lee J. Stable control of the bicycle robot on a curved path by using a reaction wheel[J]. Journal of Mechanical Science and Technology, 2015, 29 (5): 2219-2226.